Available online at www.sciencedirect.com
SCIENCE DIRECT®
International Journal of Mass Spectrometry 228 (2003) 1067–1082
International Journal of Mass Spectrometry
www.elsevier.com/locate/ijms

Mass selective photodetachment photoelectron spectroscopy: small transition metal (Fe, Ni) carbon hydrogen compounds

G. Drechsler, U. Boesl*

Institut für Physikalische und Theoretische Chemie, Technische Universität München, Lichtenbergstr. 4, 85748 Garching, Germany

Received 11 November 2002; accepted 30 April 2003

Dedicated to Professor Helmut Schwarz on the occasion of his 60th birthday.

Abstract

Photodetachment photoelectron spectra of chemical products, due to reactions between transition metals and acetylene, have been measured. These products existed as negative ions which have been mass selected in a time-of-flight analyser prior to laser photodetachment. The photoelectron spectra supply values for the electron affinity as well as energies for neutral excited electronic states and vibrations. The following complexes have been investigated: FeC_2H_x ($x = 0, 1, 2, 3$), FeC_4H_x ($x = 2, 3$), Fe_2H_x ($x = 1, 2$), NiC_2H_x ($x = 1, 3$) and NiC_4H_3. These isolated transition metal-containing complexes may correspond to surface bound intermediates during catalytic reactions of hydrocarbons on transition metal surfaces or deliver information about relevant transition metal carbon and transition metal hydrogen bonds.

Keywords: Photoelectron spectra; Photodetachment; Metal hydrocarbon compounds

1. Introduction

Transition metal compounds play an important role in different environments such as interstellar clouds near cold stars (which are sources of transition metals) [1] or hot terrestrial chemistry (e.g., plasmas or metal works). Bonds between transition metal and carbon atoms are of fundamental importance in organometallic chemistry and gained additional interest since the detection of metallocarbohedrenes (MetCars) [2]. In this context, the recent formation of metal hydrocarbon clusters (i.e., $Fe_{13}(C_2H_2)_6$ [3,4]) also is noteworthy. Small transition metal carbon hydrogen compounds are of particular importance for heterogeneous catalytic reactions of hydrocarbons on metal surfaces (e.g., acetylene on iron) [5–7]. As an example, a single acetylene molecule will react with one or few iron atoms of an iron surface and form intermediate transition complexes during the first state of reactions such as hydrogenation, dehydrogenation or polymerisation. The study of these intermediate complexes, their existence, structure and energy levels would help to shed light onto the complex and not fully understood mechanism of heterogeneous catalytic processes.

Despite powerful methods for surface studies (such as HREELS: high resolution electron energy loss spectroscopy [8,9]), the unequivocal study of these complexes on the surface is difficult or even impossible due

* Corresponding author. Tel.: +89-289-13397; fax: +89-289-14430.
E-mail address: ulrich.boesl@ch.tum.de (U. Boesl).

1387-3806/$ – see front matter © 2003 Elsevier Science B.V. All rights reserved.
doi:10.1016/S1387-3806(03)00220-3

to the mixture of species, complexes and sites on the surface. A first step to a more detailed species selective information is to form such complexes in the gas phase and study them as isolated, not surface bound species. Mass spectrometry supplies the tools to study the catalytic action of transition metal cations in carbon hydrogen chemistry [10–12]. Ion mobility spectroscopy yields information on the molecular structure of isolated ionised metal carbon species [13], in particular. Neutralisation–reionisation mass spectrometry [14,15] is one way of access to isolated not-surface bound transition metal carbon hydrogen complexes in their neutral state [16–18]. Isolation in noble gas matrices for FT-IR spectroscopy allows the study of such intermediate neutral species [19–21] even in more detail.

Photodetachment photoelectron spectroscopy (PD PES) is one of the most promising tools to study neutral isolated complexes which are not accessible by conventional means, in general (for a review see, e.g., refs. [22,23]), and neutral isolated transition metal complexes in the gas phase [24–35], in particular. The benefit of PD PES is that it can be combined with mass spectrometry giving rise to mass selected photoelectron spectra. In opposite to conventional photoelectron spectroscopy, PD PES involves transitions between negatively charged species and their neutral counterparts. In other word, PD PES supplies mass selected spectroscopic information about neutral species. In this work, PD PES spectra of the negative ions of transition metal carbon hydrogen compounds have been measured; the results on the corresponding neutral molecular species are presented here. These results are discussed in a first qualitative way. A deeper insight is only possible by a concerted theoretical and experimental investigation. Up to now, there is few theoretical work published on small transition metal hydrocarbon complexes.

2. Experimental

The apparatus has been presented in detail elsewhere [36–38], and is only shortly described here. Negative ions are formed in a pulsed supersonic beam of carrier gas seeded with acetylene. Metal atoms and electrons are supplied by laser-induced photoelectron emission and atomic desorption from a revolving disc made out of iron or nickel (purity of 99.96%), respectively. Its edge is positioned as near as possible (<1 mm) to the nozzle of the supersonic beam. For photoelectron emission, a Nd:YAG laser (532 nm, 2 mJ) is weakly focused onto the edge of the disc; its continuous rotation protects the plane metal surface from being destructed and thus allows a highly stable performance of the ion source. Since the photon energy is not far above the work function of the metal, the kinetic energy of the emitted electrons is small. This enhances direct or dissociative electron attachment. Further chemical reactions may occur in the dense region of the supersonic beam or on the metal surface. For further details of the negative ion source see ref. [37].

The whole mixture of carrier gas, neutral molecules and diverse negatively charged species then drifts down into an ion optics which represents the source of a linear time-of-flight mass analyser. A negative high voltage pulse is applied to the repelling electrode of this ion optics and the manifold of different anionic species is extracted into the field free drift region. After being collimated by electrodes of the ion optics itself as well as by a separate Einzel lens, the bunches of negative ions cross the space focus of the pulsed ion source, about 940 mm away from the point of ion extraction. This drift length is enough to separate ion bunches of different mass sufficiently. Due to their different flight times and due to the ion bunch compression in the space focus, a mass resolution of up to $R_{50\%} = 600$ can be reached. If the ion mass of interest is preceded or followed by very intense ion pulses of slightly different mass, a considerable background due to electron detachment of these unwanted ions during collisions with solid surfaces or residual gas molecules may be caused. To avoid that problem an additional pulsed mass filter is used in front of the point of photodetachment. For further details of the time-of-flight analyser see ref. [38].

In Fig. 1 mass spectra of the two classes of species, namely $Fe_nC_xH_y^-$ and $Ni_nC_xH_y^-$ are presented. A

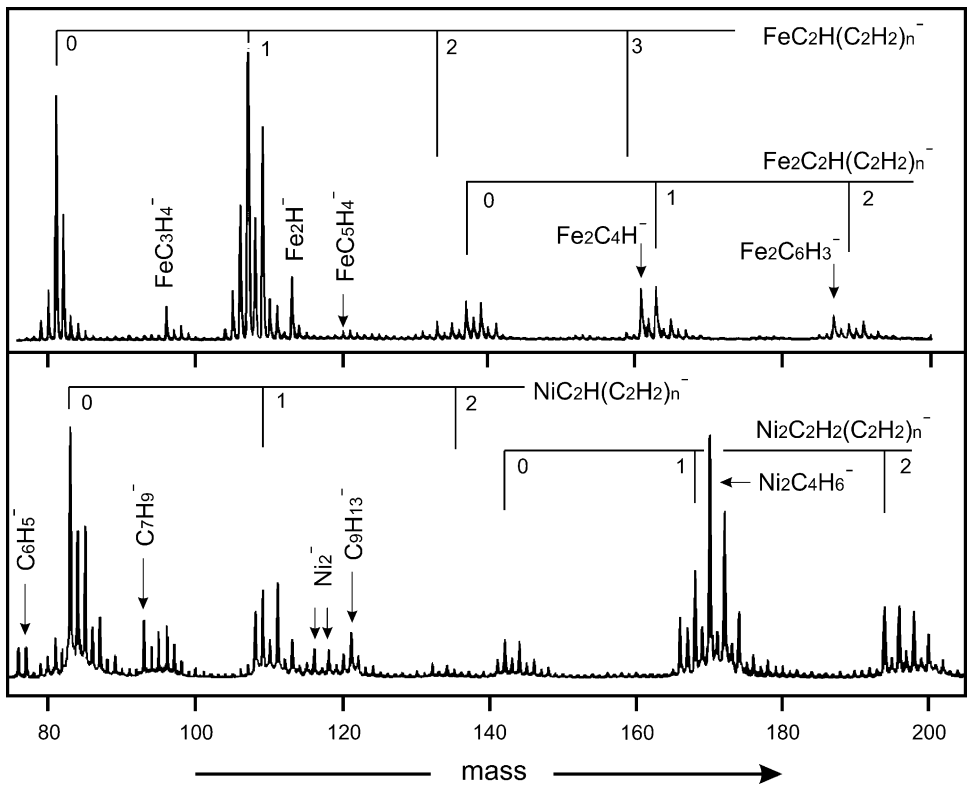

Fig. 1. Negative-ion mass spectra of products due to chemical reactions of iron or nickel with acetylene in the gas phase. Acetylene was seeded in the carrier gas of a supersonic molecular beam; transition metal atoms have been laser-ablated from a metal wire; free electrons were supplied by laser-induced photoemission from the metal wire.

laser pulse energy (Nd:YAG laser) of 2 mJ and a focal spot size of 1–0.1 mm^2 has been used. This supplied a laser intensity which is large enough for sufficient ablation of metal atoms and emission of photoelectrons from the iron or nickel surface; on the other hand, it is small enough to suppress the formation of a plasma on the metal surface. As a laser wavelength the second harmonic of the Nd:YAG laser (532 nm) has been used to avoid photofragmentation of the newly formed molecular species. It turned out that the absorption of two 532 nm photons which is necessary to surpass the work function of iron or nickel is efficient enough and does not cause further problems. Under these conditions extensive formation of reaction products of iron or nickel with acetylene and formation of carbon clusters is achieved. The density numbers of the latter has been reduced by an optimised gas mixture of the supersonic beam. A relative Ar to acetylene concentration of 0.95–0.05 has been used for the spectra presented here.

The mass spectrum at the top of Fig. 1 reveals two series of iron-containing complexes which can be characterised by $FeC_2H(C_2H_2)_n^-$ and $Fe_2C_2H(C_2H_2)_n^-$. Each series member has neighboured mass peaks due to missing or additional H atoms, e.g., $FeC_2(C_2H_2)_n^-$, $FeC_2H_2(C_2H_2)_n^-$, or $FeC_2H_3(C_2H_2)_n^-$. On the other hand, metal complexes with uneven numbers of carbon atoms are very rare or not existent at all. An interesting feature of the iron-based mass spectrum is the presence of iron hydrides Fe_2H^- and $Fe_2H_2^-$. Also in the nickel-based mass spectrum two series appear. In opposite to the Fe-containing mass peaks, the second series in the nickel-based mass spectrum is better characterised as $Ni_2C_2H_2(C_2H_2)_n^-$. Its members

show different mass patterns which are not due to the isotope ratio of nickel of 68–26% ($^{58}Ni/^{60}Ni$). The first series $NiC_2H(C_2H_2)_n^-$ behaves very similar to that of iron when taking into account the different isotope ratios of iron and nickel. Interestingly, no nickel hydrides, but nickel dimers appear in the spectrum. In addition, the production of hydrocarbons can be observed. In particular, the $C_6H_5^-$ might be of interest concerning the formation of benzene out of acetylene catalysed by metal surfaces. The strong MC_2H^- (M = Fe, Ni) peaks agree well with the strong appearance of the corresponding MC_2H^+ cations in the neutralisation–reionisation spectra [17]; this indicates particularly stable corresponding neutral species MC_2H. The appearance of the mass spectra and their patterns can be changed significantly by varying the ion source conditions, i.e., gas pressure, supersonic beam gas mixture, laser power, moving of the metal surface (same spot or fresh spots of the metal surfaces for subsequent laser shots). These possibilities have been used to enhance the negative ion peak of the species of interest for the photodetachment photoelectron spectra presented in the following sections.

The photodetachment itself is performed in the space focus of the ion source optics. The electron detaching laser pulse is focussed at this point and is exactly synchronised with the fly-by-time at which the negative ions of interest are passing the space focus. This is achieved using standard Nd:YAG lasers (or a Nd:YAG pumped dye lasers) with laser pulses of <10 ns and a jitter of <1 ns. The negative ions passing the point of detachment as well as the formed neutrals are detected by a multi-channel plates detector (MCP) placed a few centimetres behind the space focus. For discrimination of neutrals and anions, a negative high voltage is applied to a reflecting grid in front of the MCP so that negative ions cannot reach the MCP.

This is displayed in Fig. 2. On the left side a scheme of the experimental arrangement for mass selective photodetachment and discrimination of neutrals and ions is shown. On the left side mass spectra covering the mass range of $FeC_4H_x^-$ and of the cluster C_9^- are shown for the experimental conditions: (a) ion reflector off, laser off, (b) ion reflector on, laser off and (c) ion reflector on, laser on. In the latter case, neutrals are formed during the detachment process, which pass the ion reflector and are selectively detected while negative ions cannot reach the detector. Since the laser pulse was synchronised with the fly-by-time of $FeC_4H_2^-$, only the neutral complex FeC_4H_2 is formed and detected. The photodetached electrons, on the other hand, are analysed by their flight time in a drift region which is kept free of magnetic and electric fields as much as possible. Magnetic fields are shielded by a double wall μ-metal tube. Electric residual fields, which are mostly due to surface effects, are minimised by using gold plated surfaces. Photodetachment photoelectron spectroscopy is performed by applying fixed detachment wavelengths (i.e., 355, 532, 690 nm) and analysing the electron energy by a 400 mm long time-of-flight tube. The negative ion trajectory, the axis of the electron energy analyser and the direction of laser light propagation are vertical to each other and are crossing in the space focus. In addition, the polarisation of the laser light can be changed between parallel and vertical with respect to the direction of emission of the observed photoelectrons.

The photoelectron spectra presented in the next sections have been performed under various conditions exploiting two features of light: photon energy and polarisation. The variation of photon energy allows to change the speed of the emitted electrons and thus to adjust the experimental conditions for optimal resolution of photoelectron spectra in time-of-flight energy analysers. Therefore the presented photoelectron spectra are marked by the used laser wavelength 355 nm (28,200 cm^{-1} or 3.49 eV), 532 nm (18,800 cm^{-1} or 2.33 nm) and 690 nm (14,500 cm^{-1} or 1.80 eV). The variation of the laser light polarisation allows to determine if the detached electrons are released isotropically or non-isotropically (i.e., emitted s-wave, p-wave, d-wave, etc.) and therefore delivers information on the symmetry of the molecular orbital from which the electron has been released. An emitted s-wave electron is independent from photon polarisation. Consequently, such an independence

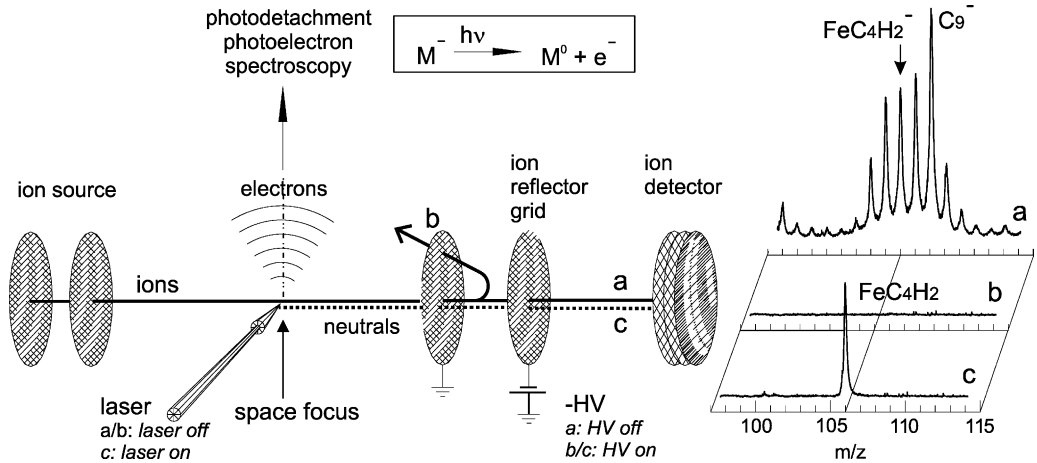

Fig. 2. Mass selective photodetachment in the space focus of the pulsed ion source of a time-of-flight mass analyser. Demonstration by three mass spectra: (a) uninfluenced negative-ion mass spectrum of FeC_4H_x and C_9; (b) anion reflecting field on (no ions reach the detector); (c) in addition to (b) electron detaching laser on and synchronised with the transit time of FeC_4H_2 (neutralised molecular compounds with mass 106 arrive at the ion detector).

indicates that the corresponding electron (due to angular momentum conservation) cannot be detached from a state with orbital angular momentum $\lambda = 0$ or a total symmetric molecular state, respectively. On the other hand, a strong dependence of the photoelectrons on the laser light polarisation is an indication for emitted p- or even higher order waves. In the former case, the corresponding bound electronic state is a s- or total symmetric state. For this reason, the photodetachment photoelectron spectra are also marked by $\parallel$ or by $\perp$ indicating if the used laser light polarisation is parallel or vertical to the direction in which the observed electrons are emitted. In addition to a characterisation of the involved electronic states, this type of experiment helps to assign a band in the spectrum to a new electronic state or to vibrational substructure (vibrational bands should show the same polarisation behaviour as their electronic origins).

3. Results

3.1. Iron-containing complexes: FeC_xH_y

In Fig. 3, anion–photoelectron spectra of the six molecular ions FeC_2^-, FeC_2H^-, $FeC_2H_2^-$, $FeC_2H_3^-$, $FeC_4H_2^-$ and $FeC_4H_3^-$ are displayed. Some results about FeC_2^-, FeC_2H^-, $FeC_2H_2^-$ have already been presented in refs. [23,34,35]. Some further details such as results due to the change of laser light polarisation will be given here. At the top of Fig. 3, the photodetachment photoelectron spectrum of FeC_2^- is shown. It exhibits the neutral X state at an electron binding energy of $15{,}955 \pm 5\,cm^{-1}$ (adiabatic electron affinity) with a broad Franck–Condon envelope of the Fe–C stretching frequency ($\nu = 557\,cm^{-1}$). This corresponds to $\omega_e = 561.6\,cm^{-1}$ with an anharmonicity of $2.1\,cm^{-1}$ [39]. A dissociation energy of about $D_0 = 37{,}000\,cm^{-1}$ or $450\,kJ\,mol^{-1}$ can be deduced from these values. The broad Franck–Condon envelope may be interpreted as a strong change of the Fe–C bond length during the neutral ← negative ion transition. Furthermore, there are two electronic states (see Fig. 11 in [23]) at excess energies of $6815\,cm^{-1}$ (A) and $8515\,cm^{-1}$ (B) which are not shown here. While band B does not show any vibrational excitation, band system A reveals a progression of the (probably) bending mode with $\nu_{vib} = 1000\,cm^{-1}$. This is an indication of a linear structure in the case of the X and B states, a non-linear structure in the case of the A state.

These numbers agree well with the PD PES spectrum of Li and Wang [33]. Due to application of

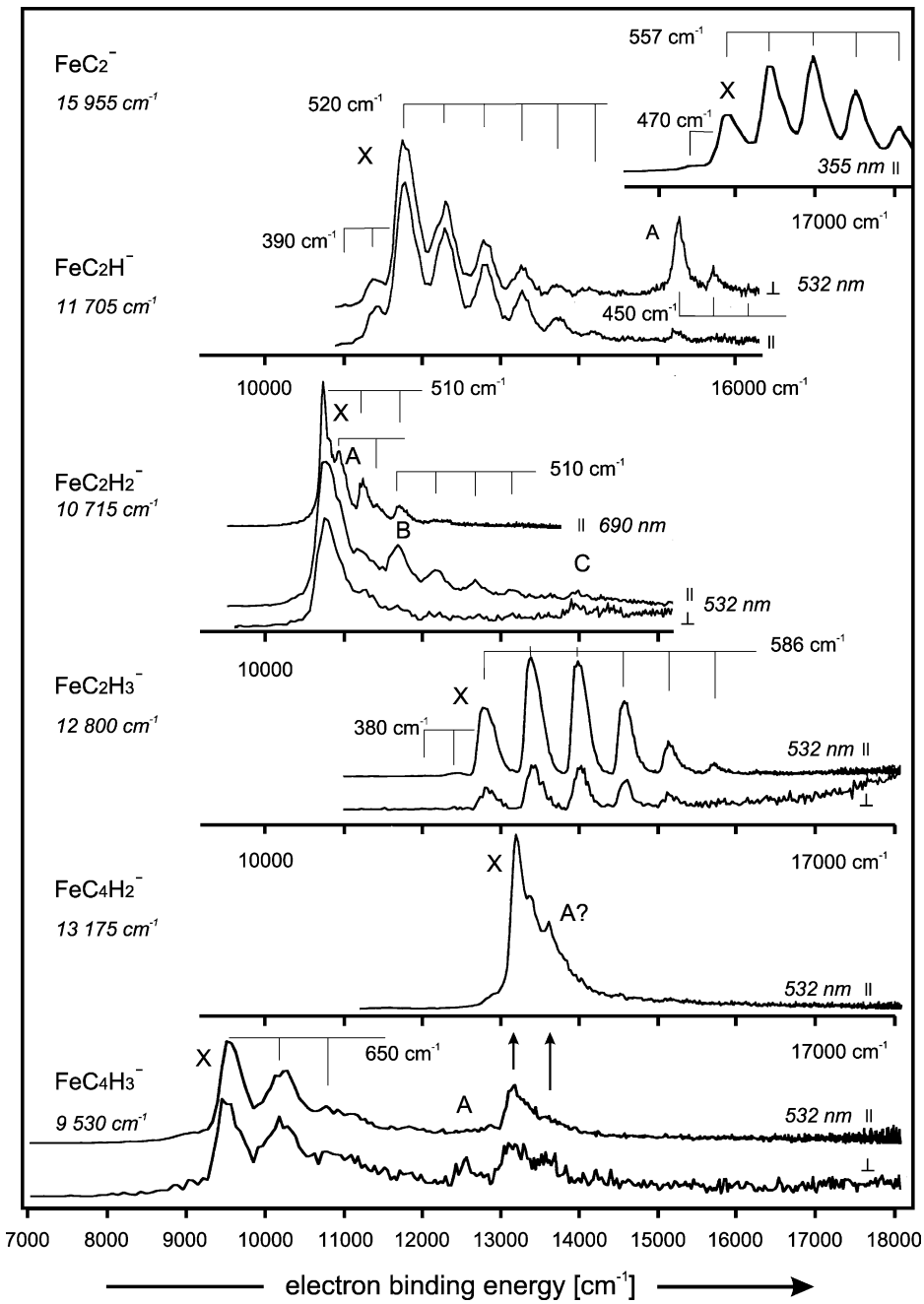

Fig. 3. Photodetachment photoelectron spectra of FeC_xH_y ($x = 2, 4$; $y = 0, 1, 2, 3$). For each iron carbon hydrogen complex the electron affinity is given. The PD PES spectra are marked with the wavelength and the polarisation of the used photodetaching laser light. Vibrational progressions are characterised by lines and the energy of their first vibrational quantum. Tentatively assigned excited electronic states are marked by A, B, or C.

anion-ZEKE spectroscopy [34,35] the electron affinity and the vibrational values for the neutral ground state given above have been determined with considerably higher accuracy. In addition, the resolution of the PD PES spectra [23,34,35] in the range above 22,000 cm^{-1} is higher and our assignments of A and B states are different from theirs. There exist some theoretical work about FeC_2 [40,41]. Both predict a circular structure for the lowest electronic state of the neutral species. In one paper [41], even a circular structure of the anionic ground state is predicted. From ion mobility experiments [13], a circular structure for FeC_n^- ($n = 7$), a coexistence of linear and circular structure for FeC_n^- ($n = 5, 6$ and 8), but a linear structure for FeC_4^- have been determined. A linear structure for the small clusters FeC_n^- ($n = 2, 3$) may be deduced from these results which would be in opposite to one of the theoretical predictions. A cyclic–cyclic transition is not supported by the experiment, since the theoretically predicted C–Fe stretching vibrations for the cyclic neutral and the cyclic anionic FeC_2 isomers are 385 and 498 cm^{-1} [41], respectively, in opposite to the experimental values of 557 and 480 cm^{-1} (hot band in Fig. 3). A linear ← cyclic transition is not evident from the PD PES spectra. In this case one would expect the appearance of further vibrations and not exclusively of the Fe–C stretching mode. We therefore prefer the interpretation of the X band in our experimental PD PES spectra of FeC_2^- as a linear–linear transition with a linear anionic and a linear neutral ground state.

The case of FeC_2H^- bears great resemblance to FeC_2^- at the first glance indicating a linear ← linear transition in this case, too. A pronounced progression structure of the X state with a frequency of ν(Fe–C) = 520 cm^{-1} appears. Both Fe–C stretching frequency and Franck–Condon envelope indicate a somewhat less strong change of Fe–C bond strength and bond length than in the case of FeC_2. However, the adiabatic electron affinity (11705 ± 20 cm^{-1}) as well as the excess energy of the A state (which shows a strong dependence on polarisation in opposite to the X state) have drastically decreased, while the B band (see Fig. 11 in ref. [23]) has the same shape and excess energy as the corresponding analogue of FeC_2. However, in FeC_2 (assuming the structure Fe–C≡C–) the ground state of iron (^5D, $3d^64s^2$) and the two singly occupied σ_{sp} orbitals of –C≡C– form the electron configuration $3d^6\sigma^2\sigma_{sp}^2$ of the linear neutral ground state. Such an electron configuration is not possible with FeC_2H. The ^5D ($3d^64s^2$) state of iron and the residual singly occupied σ_{sp} orbital of –C≡C–H would result in a $3d^6\sigma^2\sigma^{*1}$ electron configuration of the neutral ground state and a $3d^6\sigma^2\sigma^{*2}$ in the negative ion. Due to two electrons with anti-bonding character this would correspond to a very weakly bound or even unstable configuration which is in opposite to the strong mass speak of FeC_2H^- in the mass spectrum. Much more probable therefore is that the excited ^5F ($3d^74s^1$) state of iron contributes to a $3d^7\sigma^2$ ground state configuration of the neutral and to a $3d^7\sigma^2\sigma^{*1}$ of the negatively charged FeC_2H complex. This would be in agreement with a neutral as well as anionic linear structure: Fe–C≡C–H (similarly to FeC_2 and in opposite to a vinylidene structure Fe–H≻C=C=) and would explain the comparable vibrational substructure of the neutral X states as well as the strongly reduced frequency of 390 cm^{-1} of the hot band (vibration initially excited in the negative ion) which is due to a weak Fe–C bond in the negative ion. A linear acetylide structure has also been supported by neutralisation–reionisation experiments [17]. The electron binding energies of the X, A, B and C states given above agree with corresponding values from earlier PD PES spectra (no vibrations resolved) [29] within a few 100 cm^{-1}.

The situation is quite different for FeC_2H_2. The electron affinity (10,715 cm^{-1}) decreased even further. The Franck–Condon envelope of the first band system fails to show a clear progression, which indicates a minor change of the molecular structure between anionic and neutral ground states. On the other hand, it exhibits a complex substructure which might be due to low energetic excited electronic states or other isomers. The excess energies of the corresponding bands (tentatively assigned as A and B states) have excess energies of only 215 and 1000 cm^{-1}, respectively, and exhibit weak progressions with a vibrational frequency of 510 cm^{-1}, similar to the X

band. A further weak band C, also assigned to an electronic state, appears at 3240 cm^{-1} excess energy. In addition, a strong D band at 14,800 cm^{-1} has been found (see Fig. 11 in [23]). The origins X, A, B and C show quite different behaviour for vertically and horizontally polarised laser light (X and A show a minor change, B and C a strong but opposite change) which is typical for electronic states with different symmetry and supports the tentative assignment of A, B and C as excited electronic states. The common vibrational frequency of 510 cm^{-1}, however, indicates a molecular structure with a strong Fe–C bond, similar to the Fe–C≡C– structure of FeC_2 and FeC_2H. The structure Fe···H–C≡C–H, which has been observed by FT-IR matrix spectra [20], would not give rise to a Fe–C vibration at 500 cm^{-1}, in opposite to the linear structure H–Fe–C≡C–H. This structure has been suggested to be formed as a photo-product after irradiation of the noble gas matrix with laser light (280–360 nm) [42]; this suggestion has been made on the basis of further matrix isolation FT-IR studies.

In contrast to $FeC_2H_x^-$ ($x = 0, 1, 2$), the complex $FeC_2H_3^-$ cannot be formed by a simple reaction of iron atoms and acetylene. Collisions between compounds already formed in the gas beam have to occur. A probable process is the collision of iron hydride with acetylene although FeH^- is not found in the mass spectrum; however, this may be due to missing possibilities of fast energetic stabilisation. The complexes Fe_2H^- and $Fe_2H_2^-$ are present in the mass spectrum very well. The PD PES spectrum of $FeC_2H_3^-$ exhibits an exceptionally clear and distinct progression of the neutral X state with a Franck–Condon envelope similar to that of the FeC_2 X state. No low-energetic excited electronic states within the next 5000 cm^{-1} are found. The adiabatic electron affinity is 12,800 cm^{-1}. The strong signal decrease by a factor of seven for vertical polarisation is clearly due to a p-wave electron emission; this is an indication that the additional electron of the negative ion may stem from a s or d orbital (probably from the iron as supported from the strong Fe–C vibrational progression). The vibrational energy of 586 cm^{-1} is the largest of all FeC_2H_y compounds, presented up to now. In addition, the anharmonicity is too small to be determined; this is a further argument for a very strong Fe–C bond. One possible structure is mono-iron ethylene (FeH≻C=C≺H_2); however, a Fe–C vibrational energy of 507 cm^{-1} has been found [19] for the product of an insertion reaction of iron and ethylene. An other structure, which would well correspond to the particularly strong Fe–C bond, is H–Fe=C=C≺H_2.

The following two complexes FeC_4H_2 and FeC_4H_3 are due to reactions of the basic compounds $FeC_2H_x^-$ ($x = 0, 1, 2$) and one acetylene molecule. The nearly complete missing of $FeC_xH_y^-$ with uneven numbers of carbon atoms confirms the suggestion that the formation of these metallo-organic compounds is due to basic –C≡C– elements. The PD PES spectrum of $FeC_4H_2^-$ shows great similarity with the FeC_2H_2 spectrum, although the electron affinity is 13,175 cm^{-1} and thus considerably larger. The missing vibrational substructure indicates a minor structural change between anionic and neutral structure as in the case of FeC_2H_2. Obviously, the extra electron of the negative ion occupies a nonbonding orbital. Two minor peaks appear at the high energy wing of the single band in the spectrum, one at 175 cm^{-1}, the other at 435 cm^{-1}. They seem to be due to electronic substructure or other isomers rather than to vibrational structure. The PD PES spectrum $FeC_4H_3^-$ exhibits a very different pattern: the wide Franck–Condon envelope is an argument for a strong change of the Fe–C bond length. In addition, the very large frequency of 650 cm^{-1} (compared with 510–586 cm^{-1} in the other spectra) might be a hint for a –C–Fe–C– bond with a strong force constant for the anti-symmetric –C–Fe–C– or even –C–Fe=C– stretching mode. Having the argument of the basic –C≡C– elements in mind, a possible structure of FeC_4H_3 could be: H–C≡C–Fe=C=CH_2. The electron affinity of only 9530 cm^{-1} (the smallest in Fig. 3) is a further argument for a strongly bound iron atom in the neutral complex and a very loosely bound extra electron (at the iron atom) of the negatively charged complex.

These results on iron carbon hydrogen compounds still leave many questions open. Thus it is not clear, whether in some spectra of Fig. 3 spectral features

which have been assigned to low lying electronically excited states in reality are due to isomeric structures. This becomes even more a question since high resolution PE spectra of FeC_2 and FeC_2H (anion-ZEKE spectroscopy) [34,35] revealed fine structure (splitting of the X band progression with intervals of some 100 cm^{-1}) whose origin is not yet understood. One possible explanation is spin orbit splitting due to the involved d electrons. In addition, even cyclic structures of the neutral and anionic ground states cannot be excluded, for instance in the case of the neutral FeC_4H_3 complex with its large Fe–C frequency of 650 cm^{-1}.

3.2. Iron hydrides: Fe_2H and Fe_2H_2

Metal cluster hydrides have been investigated using a large variety of experimental and theoretical methods [24,26–28,43–49]. The idea behind these studies is that these complexes represent the most simple models for dissociative chemisorption of hydrogen to transition metal surfaces. PD PES has been involved to study isolated metal hydrides excluding interaction with carrier substances, ligands, etc. One tried to obtain information about these processes by a comparison of pure metal clusters, metal hydrides and metal cluster hydrides. An interesting example is chromium. An electron affinity of 4073 cm^{-1} and a Cr–Cr vibration of 452 cm^{-1} for Cr_2 has been measured [28], as well as an electron affinity of 4541 cm^{-1} and a Cr–H vibration of 1472 cm^{-1} in the case of Cr–H, and finally an electron affinity of 11,889 cm^{-1}, a Cr–Cr vibration of 554 cm^{-1}, a Cr–H vibration of 1571 cm^{-1} and a Cr–Cr–H bending vibration of 215 cm^{-1} in the case of Cr_2H [27]. While in Cr_2 and Cr_2H, respectively, the d electrons are responsible for the metal bond and the two s electrons of the two metal atoms for the metal hydrogen bond, the situation is much more complex in iron cluster hydrides. In the iron dimer, the bond is preferentially due to the s orbitals with small contribution of the d orbitals [25]. For an additional Fe–H bond, d electrons have to be involved more strongly which should result in a significant change of the electronic structure in comparison to the Cr_2/Cr_2H system. For Fe_2, FeH and FeH_2 PD PES spectra have already been measured supplying the following numbers for Fe_2 [25]: EA 7275 cm^{-1}, ν(Fe–Fe) 300 cm^{-1}; for FeH [24]: EA 7533 cm^{-1}, ν(Fe–H) 1774 cm^{-1}; and for FeH_2 [26]: EA 8461 cm^{-1}. In Fig. 4, the PD PES spectra of Fe_2H and Fe_2H_2 are now presented.

For Fe_2H two spectra are shown in Fig. 4, a wide-range low-resolution (355 nm laser detachment wavelength) and a low-energy high-resolution spectrum (690 nm). An adiabatic electron affinity as small as 4550 cm^{-1} has been observed as well as bands marked with a, b and c with excess energies of 1150, 3725 and 8450 cm^{-1}, respectively. In the high resolution spectrum very weak structures at 2000, 2500 and 3000 cm^{-1} appear which might indicate a vibrational progression with unknown origin. The strong bands a, b and c can only be explained by excited electronic states due to their large excess energies above the origin of the X state. The absence of vibrational progressions for all of the bands X, a, b and c is significant. The spectrum of Fe_2H_2 in Fig. 4 is quite different. The electron affinity has increased up to 7600 cm^{-1}, and is comparable to that of Fe_2 and FeH, again. The neutral electronic ground state exhibits a clear and strong vibrational progression with a fairly large vibrational energy of 550 cm^{-1}. There is a second band system with a nearly as large vibrational energy of 530 cm^{-1} and its origin at 2900 cm^{-1}. The energy of 2900 cm^{-1} is larger by a factor of at least 1.7 in comparison to all other Me–H vibrational constants. Therefore, band system A is assigned to an excited electronic state. Finally, the 550 cm^{-1} vibration can only be explained by a Fe–Fe vibration. The increase of its energy in comparison to the 300 cm^{-1} of Fe_2 [25] is a further hint for the inclusion of d electrons in the case of additional Fe–H bonds and thus a strengthening of the metal bond in the presence of the hydride bond. The Franck–Condon envelope tells one that the detached electron is emitted from an orbital with anti-bonding character for the metal bond.

3.3. Nickel-containing complexes: NiC_xH_y

Nickel and iron atoms differ by their number of valence electrons. This gives rise to different electron

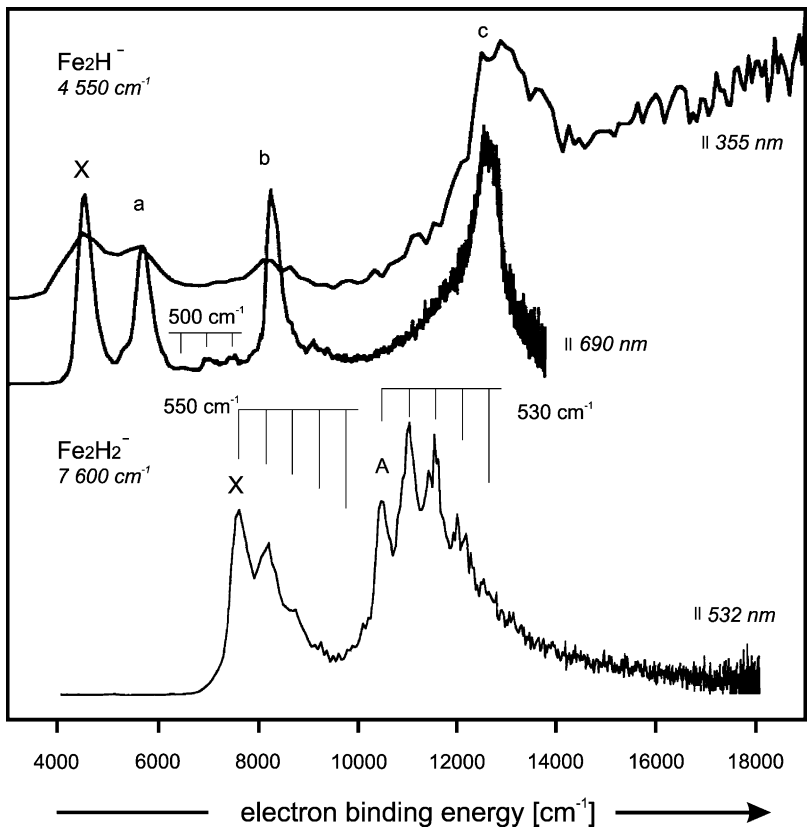

Fig. 4. Photodetachment photoelectron spectra of iron hydrides Fe_2H and Fe_2H_2. Values for the electron affinity, vibrational energies and the wavelength of the photodetaching laser are given. ||: Polarisation of laser light with respect to the direction of flight of the observed photoelectrons (see Fig. 2).

configurations in their ground states: ^5D ($3d^64s^2$) for iron and ^3F ($3d^84s^2$) for nickel [50]. The lowest electronically excited states not only differ by their electron configuration but also their energy. The first excited state ^5F ($3d^74s^1$) of iron lies at 859 meV; the first and second excited state of nickel with the configuration $3d^94s^1$ have considerably lower energies: 25 meV for the ^3D ($^3F_4 \rightarrow {}^3D_3$) state and 422 meV for the ^3D ($^3F_4 \rightarrow {}^1D_2$) state. Compounds of nickel therefore should be characterised by strong configuration interaction of these closely neighboured electronic states. This might be the reason for the different appearance of the PD PES spectra of nickel- and iron-alkyl compounds. The spectra of most iron-alkyl compounds in Fig. 3 are clearly dominated by the Fe–C stretching mode. In the PD PES spectra of the corresponding nickel compounds a number of different modes appear, such as the C–H, C–C and Ni–C stretching vibration. The following vibrational frequencies obtained from FT-IR spectroscopy are of special benefit for the interpretation of the Ni-alkyl PD PES spectra. C–H stretching frequencies of 3287 and 3288.5 cm^{-1} for C_2H_2 in the gas phase [51] and in the Ar matrix [20], respectively, and of 3112 cm^{-1} for $Ni(C_2H_2)$ in the Ar matrix [52] have been found. In the latter system, also a –C≡C– stretching mode of 1729 cm^{-1} and a Ni–C stretching mode of 570 cm^{-1} [52] have been measured.

In Figs. 5 and 6, PD PES spectra of NiC_2H^- are presented. The spectra of Fig. 5 have been performed

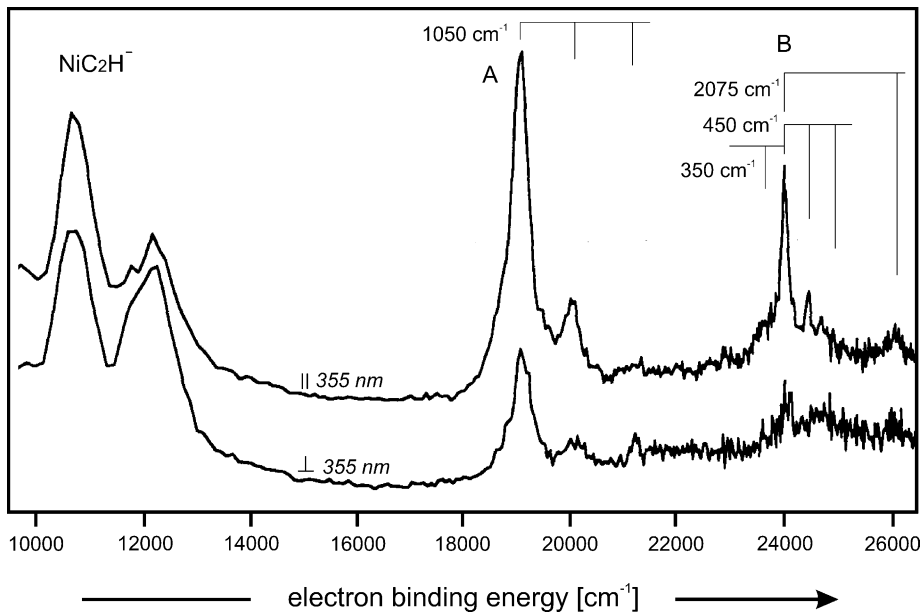

Fig. 5. Photodetachment photoelectron spectra of NiC_2H with marked vibrational progressions and vibrational energies. The photodetaching laser wavelength was 355 nm (~28,170 cm^{-1}). ⊥, ||: Polarisation of laser light with respect to the direction of flight of the observed photoelectrons (see Fig. 2). For better resolved X-state spectrum see next figure.

with a detaching laser wavelength of 355 nm and two different polarisations. For a better resolution of the range of small electron binding energy (which corresponds to a high kinetic energy of the detached electrons), spectra with a detaching laser wavelength of 532 nm have been measured as presented in Fig. 6. The change of polarisation in Fig. 5 from parallel to vertical strongly reduces the intensity of the two band systems A and B, which therefore are assigned as two excited states with their vibrational progressions. The band system around and below 10,000 cm^{-1} (which is assigned to the X state, see Fig. 6) rather shows a slight enhancement than a strong reduction. State A exhibits a vibration of about 1050 cm^{-1} which could be due to a C–C–H bending mode. The B state shows a vibration at 450 cm^{-1} which is characteristic for a Ni–C stretching mode and one at about 2075 cm^{-1} which may be attributed to a –C≡C– stretching mode. The range of electron binding energy from 6000 to 18,000 cm^{-1} is displayed in Fig. 6 at higher resolution. The band system of lowest energy starts at 8575 cm^{-1}, which therefore is assigned as the adiabatic electron affinity of NiC_2H. The progression of 500 cm^{-1} can be attributed to a Ni–C stretching mode. The next fairly intense band lies at 2060 cm^{-1} with an indication of a 450 cm^{-1} progression. Frequencies around 2000 cm^{-1} lie in the range of –C≡C– stretching modes.

However, this assignment is questioned by the second spectrum in Fig. 6 (polarisation changed to vertical) which does not show a uniform dependence of all these bands on the polarisation. The band near 10,600 cm^{-1} shows a reduced intensity in relation to the most other peaks. The band near 11,700 cm^{-1}, on the other hand, shows a relative enhancement. One explanation is that at these two positions electronic states interfere with vibrational bands of the ground state. The increased resolution of all bands at vertical polarisation, in particular those near the origin of 8575 cm^{-1}, indicate, however, that two similar vibronic band systems are overlapping, which may be due to two closely neighboured electronic components of different symmetry. These two components may be separated by 100 cm^{-1} or less, show slightly different vibrational frequencies, and are subject to

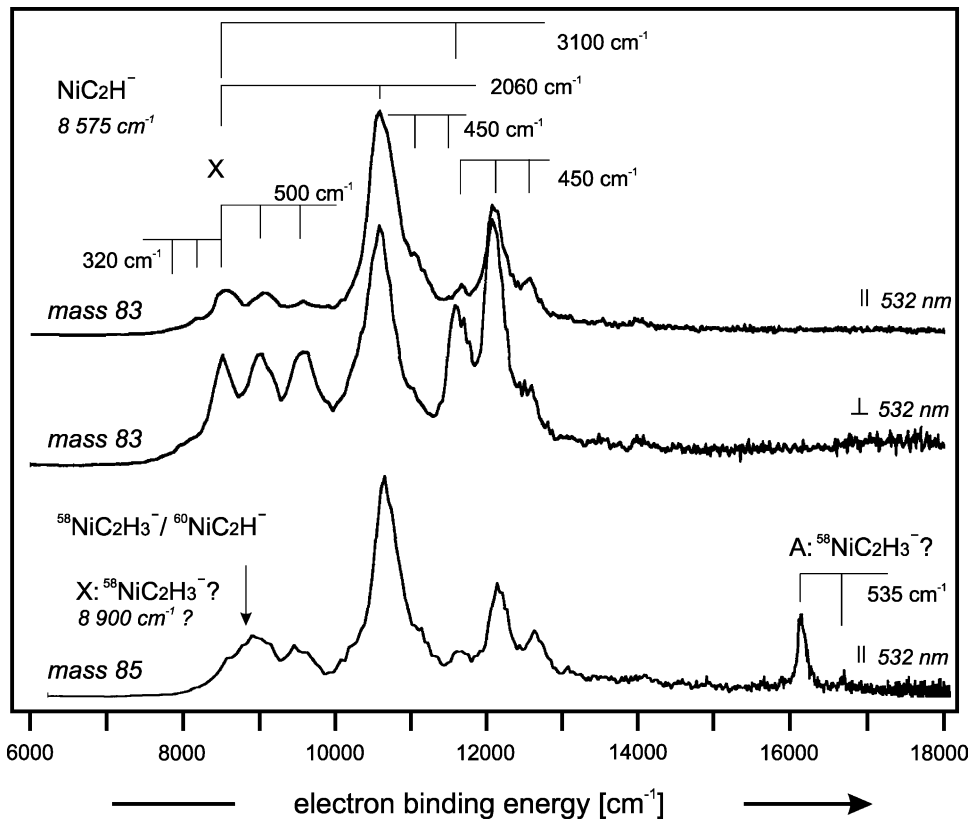

Fig. 6. Photodetachment photoelectron spectra of NiC_2H and NiC_2H_3 with values for electron affinity and vibrational energies. The photodetaching laser wavelength was 532 nm (~18,800 cm^{-1}). ⊥, ||: Polarisation of laser light with respect to the direction of flight of the observed photoelectrons (see Fig. 2). The mass 85-selective spectrum is due to the two isobar species: $^{60}NiC_2H$ and $^{58}NiC_2H_3$.

different Franck–Condon factors and Franck–Condon envelopes, respectively. Thus excitation of a possible –C≡C– stretching mode with 2060 cm^{-1} might be enhanced for the one electronic component, excitation of a possible –C–H stretching mode with 3100 cm^{-1} in the other one. The slight shift of the bands near 11,700 cm^{-1} when changing the polarisation seems to support this interpretation.

Considering possible molecular structures of NiC_2H, two very probable ones are Ni–C≡C–H and H–Ni–C≡C. Further structures are possible after rearrangements of charges and of the single hydrogen atom. However, large charge separation over short distances makes these structures rather improbable. The appearance of a –C≡C– stretching vibration favours the two structures mentioned above; finally, the appearance of a C–H stretching mode is only possible for the Ni–C≡C–H structure. We therefore assume that it is this molecular structure which causes the pattern of the PD PES spectra in Figs. 5 and 6. In the nickel acetylide structure, the nickel atom may be present in its ground state ^3F ($3d^8 4s^2$) and form a $3d^8\sigma^2\sigma^{*1}$ configuration [53] with the singly occupied sp orbital of –C≡C–H. In addition, the 3d π-orbitals of nickel may interact with the occupied –C≡C– π-orbitals and thus strengthen the Ni–C bond, which is weakened by the anti-bonding σ* molecular orbital. Another possibility is that the nearby ^3D ($3d^9 4s^1$) state of nickel gives rise to a $3d^9\sigma^2$ molecular configuration with a much stronger Ni–C σ-bond. The existence of relevant stable negative ions supplies further arguments supporting one of these two

configurations: the NiC_2H^- peak is the strongest of the $NiC_2H_x^-$ ($x = 0, 1, 2, \ldots$) group in the mass spectrum (see Fig. 1). An additional electron in the former configuration would result in a probably unstable $3d^8\sigma^2\sigma^{*2}$ configuration in the negative ion. We therefore favour the $3d^9\sigma^2$ configuration for NiC_2H.

In Fig. 6 at the bottom, a third PD PES spectrum is shown which has been measured within the ion flight time window (see Fig. 2) of mass 85 rather than of mass 83. Peaks at mass 85 can be attributed to $NiC_2H_3^-$ as well as to the isotope substituted $^{60}NiC_2H^-$. Since the isotope ratio $^{58}Ni/^{60}Ni$ is 0.68/0.26, the major part of the mass 85 peak is due to $^{60}NiC_2H^-$. This situation is reflected in the lower PD PES spectrum: the spectral structures of the upper spectrum (mass 83) within the energy range 8000–14,000 cm^{-1} re-appears in the mass 85 spectrum. By the way, this is an reinsurance that the assignment of the mass 83 peak to $^{58}NiC_2H^-$ is correct. However, there appear additional structures in the mass 85 spectrum with no bands corresponding to them in the mass 83 spectrum. These are a little bump at 8900 cm^{-1} and a line at 16,140 cm^{-1} with a small accompanying band at $+535\,cm^{-1}$. We tentatively assign these to the neutral ground state (adiabatic electron affinity) and the first excited state (A) of the neutral species $^{58}NiC_2H_3^-$, respectively. The small band at $+535\,cm^{-1}$ then corresponds to the excitation of one vibrational quantum in the A state; this vibration is tentatively attributed to a Ni–C stretching mode with a fairly high frequency (exceptional strong Ni–C bond).

Finally, Fig. 7 displays a mass selected PD PES spectrum of $NiC_4H_3^-$. The peak at 6650 cm^{-1} is assigned to the X state; it shows an additional vibrational band at about $+1100\,cm^{-1}$. The band at 10,320 cm^{-1} is attributed to the first excited electronic state of the neutral NiC_4H_3. It is accompanied by an indicated progression with a vibrational frequency of 490 cm^{-1} and a vibrational band at $+1250\,cm^{-1}$. A third much more intense and broad vibronic structure starts near 13,000 cm^{-1}. It exhibits a marked vibrational progression with a significant anharmonicity and with a Franck–Condon envelope whose maximum lies at three vibrational quanta. The first vibrational quantum of this progression has a frequency of 925 cm^{-1}; the corresponding frequency ω_e is 1079 cm^{-1}; the anharmonicity $\omega_e x_e$ is 77 cm^{-1}. In addition, a weak progression is indicated with a vibrational frequency of roughly 600 cm^{-1}. In summary, this spectrum does

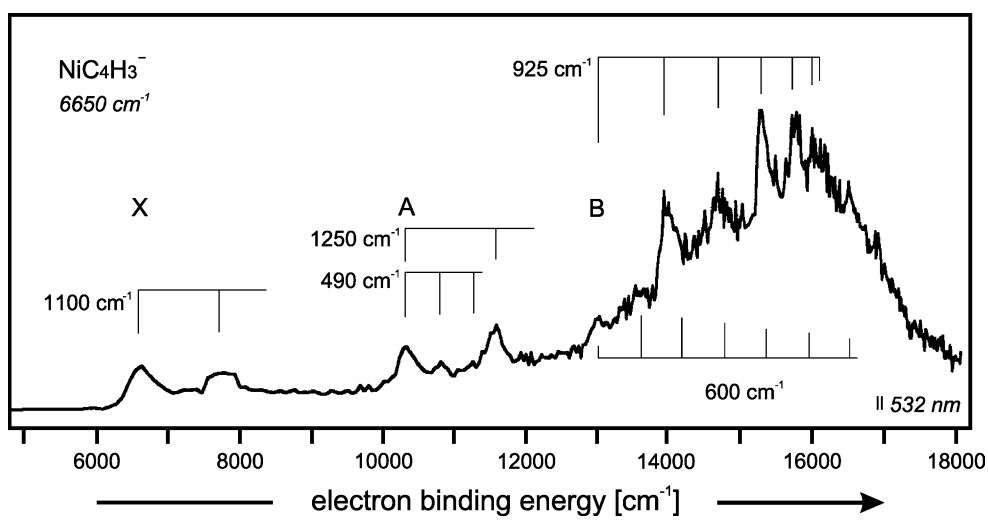

Fig. 7. Photodetachment photoelectron spectra of NiC_4H_3 with values for electron affinity and vibrational energies. The photodetaching laser wavelength was 532 nm, its polarisation was parallel with respect to the direction of flight of the observed photoelectrons (see Fig. 2).

Table 1
Summary of results: adiabatic electron affinities, excess energies of excited electronic states and vibrational energies

Molecular system	Electron affinity (cm^{-1})	Excess energy	Electronic states	Vibrational structure and vibrational energy, ν/ω_e (see ref. [39])
FeC_2	15955 ± 5	Ground state: X	$3d^6\sigma^2\sigma_{sp}{}^2$	ν(Fe–C) = 557 cm^{-1}, ω_e(Fe–C) = 561.6 cm^{-1}, $\omega_e x_e$ = 2.1 cm^{-1}, D_e(Fe–C) = 37,550 cm^{-1}, hot band ($FeC_2{}^-$: ν(Fe–C) = 470 cm^{-1})
		A: 6815 cm^{-1}	$3d^6\sigma^2\sigma_{sp}{}^2\sigma^{*1}\pi^3$	ν = 1000 cm^{-1}
		B: 8515 cm^{-1}	$3d^6\sigma^2\sigma_{sp}{}^1\sigma^{*1}$	No vibrational progression
FeC_2H	11705 ± 20	Ground state: X	$3d^7\sigma^2$	ν(Fe–C) = 520 cm^{-1}, ω_e(Fe–C) = 530.7 cm^{-1}, $\omega_e x_e$ = 4.4 cm^{-1}, D_e(Fe–C) = 16,000 cm^{-1}, hot band (FeC_2H^-: ν(Fe–C) = 390 cm^{-1})
		?: 163 cm^{-1}	Electronic state?	ν(Fe–C) = 492 cm^{-1}
		A: 3525 cm^{-1}		ν(Fe–C) = 450 cm^{-1}
		B: 9055 cm^{-1}	$3d^6\sigma^2\sigma^{*1}$	No vibrational progression
		C: 12,675 cm^{-1}		ν(Fe–C) = 480 cm^{-1}
FeC_2H_2	10715 ± 150	Ground state: X		ν(Fe–C) = 510 cm^{-1}
		A: 215 cm^{-1}	Or isomer?	ν(Fe–C) = 510 cm^{-1}
		B: 975 cm^{-1}	”	ν(Fe–C) = 510 cm^{-1}
		C: 3240 cm^{-1}	”	ν(Fe–C) ∼ 500 cm^{-1}
		D: 14,800 cm^{-1}	”	ν = 200 cm^{-1}
FeC_2H_3	12800 ± 150	Ground state: X		ν(Fe–C) = 586 cm^{-1} (very harmonic), hot band ($FeC_2H_3{}^-$: ν(Fe–C) = 380 cm^{-1})
FeC_4H_2	13175 ± 150	Ground state: X		Structure at 175 and 435 cm^{-1} (A?)
FeC_4H_3	9530 ± 150	Ground state: X		ν(Fe–C) = 650 cm^{-1}
		A: 12,585 cm^{-1}		
Fe_2H	4550 ± 150	Ground state: X	Additional peaks at the excess energies 1150 cm^{-1} (a), 3725 cm^{-1} (b), 8450 cm^{-1} (c), 16,450 and 21,750 cm^{-1} vibrational structure (?) at 2000, 2500, 3000 and 4710 cm^{-1}	
Fe_2H_2	7600 ± 150	Ground state: X		ν(Fe–Fe) = 550 cm^{-1}
		A: 2900 cm^{-1}		ν(Fe–Fe) = 530 cm^{-1}
NiC_2H	8575 ± 150	Ground state: X	$3d^9\sigma^2$ (congested by overlapping electronic components)	ν(Ni–C) = 500 cm^{-1}, ν(C–C) = 2060cm^{-1}, ν(Ni–C) = 450 cm^{-1}, ν(C–H) = 3100 cm^{-1}, ν(Ni–C) = 450 cm^{-1}, hot band (NiC_2H^-: ν(Fe–C) = 320 cm^{-1})
		A: 10,930 cm^{-1}		ν(Ni–C–C) = 1050 cm^{-1}
		B: 15,450 cm^{-1}		ν(Ni–C) = 450 cm^{-1}, ν(C–C) = 2075 cm^{-1}
NiC_2H_3	8900 ± 150	Ground state: X		Congested by $^{60}Ni^{12}C_2H$ bands
		A: 7240 cm^{-1}		ν(Ni–C) = 535 cm^{-1}
NiC_4H_3	6650 ± 150	Ground state: X		ν = 1100 cm^{-1}
		A: 3670 cm^{-1}		ν_1 = 490 cm^{-1}, ν_2 = 1250 cm^{-1}
		B: 6450 cm^{-1}		ν_1 = 600 cm^{-1}, ν_2 = 929 cm^{-1} (ν_2:ω_e = 1079 cm^{-1}, $x_e\omega_e$ = 77 cm^{-1})

not reveal a clear Ni–C stretching mode as in NiC_2H_x ($x = 1, 3$) but is rather dominated by vibrational modes which may be attributed to carbon–hydrogen vibrations (e.g., a $>C{=}CH_2$ out of plane mode whose frequency is around $1000\,cm^{-1}$).

4. Summary

Mass selected photodetachment photoelectron spectra of FeC_xH_y, Fe_2H_x and NiC_xH_y are presented. Since the final state of photodetachment are neutral systems, these spectra provide spectroscopic data about neutral vibronic states in addition to their electron affinity. Low-lying electronic states dominate the appearance of the most of these molecular systems due to the transition metals involved. In some cases the presence of particular vibrational modes allow assumptions about the most probable molecular structures. Variation of the laser light polarisation supplies further arguments for assignment of the spectra. The observed spectroscopic data are summarised in Table 1. For a satisfying interpretation of these data, however, fundamental theoretical support is necessary.

References

[1] A.J. Merer, Annu. Rev. Phys. Chem. 40 (1989) 407.
[2] B.C. Guo, K.P. Kerns, A.W. Castleman, Science 255 (1992) 1411.
[3] F. Huisken, B. Kohn, R. Alexandrescu, I. Morjan, J. Chem. Phys. 113 (2000) 6579.
[4] L.C. Cune, M. Apostel, Chem. Phys. Lett. 344 (2001) 287.
[5] K. Ziegler, E. Holzkampf, H. Breil, H. Martin, Angew Chem. 67 (1955) 541.
[6] G. Natta, J. Polym. Sci. 16 (1955) 143.
[7] R.P. Quirk, Transition Metal Catalyzed Polymerizations, Cambridge University Press, Cambridge, 1988.
[8] S.S. Perry, G.A. Somorjai, Anal. Chem. 66 (1994) 403A.
[9] S.L. Bernasek, Annu. Rev. Phys. Chem. 44 (1993) 265.
[10] D. Schröder, C. Heinemann, W. Koch, H. Schwarz, Pure Appl. Chem. 69 (1997) 273.
[11] R. Wesendrup, H. Schwarz, Organometallics 16 (1997) 461.
[12] B.C. Guo, A.W. Castleman, J. Am. Chem. Soc. 114 (1992) 6152.
[13] G. von Helden, N.G. Gotts, P. Maitre, M.T. Bowers, Chem. Phys. Lett. 227 (1994) 601.
[14] F.W. McLafferty, Science 247 (1990) 925.
[15] N. Goldberg, H. Schwarz, Acc. Chem. Res. 27 (1994) 347.
[16] C.B. Lebrilla, T. Drewello, H. Schwarz, Organometallics 6 (1987) 2268.
[17] T. Drewello, H. Schwarz, Chem. Phys. Lett. 171 (1990) 5.
[18] D. Schröder, D. Sülzle, J. Hrusak, D.K. Böhme, H. Schwarz, Int. J. Mass Spectrom. Ion Process. 110 (1991) 145.
[19] Z.H. Kafafi, R.H. Hauge, J.L. Margrave, J. Am. Chem. Soc. 107 (1985) 7550.
[20] E.S. Kline, Z.H. Kafafi, R.H. Hauge, J.L. Margrave, J. Am. Chem. Soc. 107 (1985) 7559.
[21] D.W. Ball, R.G.S. Pong, Z.H. Kafafi, J. Am. Chem. Soc. 115 (1993) 2864.
[22] J.P. Maier (Ed.), Ion and Cluster Ion Spectroscopy and Structure, Elsevier, Amsterdam, 1989.
[23] U. Boesl, W.J. Knott, Mass Spectrom. Rev. 17 (1998) 275.
[24] A.E. Stevens, C.S. Feigerle, W.C. Lineberger, J. Chem. Phys. 78 (1983) 5420.
[25] D.G. Leopold, W.C. Lineberger, J. Chem. Phys. 85 (1986) 51.
[26] A.E.S. Miller, C.S. Feigerle, W.C. Lineberger, J. Chem. Phys. 84 (1986) 4127.
[27] A.E.S. Miller, C.S. Feigerle, W.C. Lineberger, J. Chem. Phys. 87 (1987) 1549.
[28] S.M. Casey, D.G. Leopold, Chem. Phys. Lett. 201 (1993) 205.
[29] J. Fan, L.-S. Wang, J. Phys. Chem. 98 (1994) 11814.
[30] J. Fan, L. Lou, L.-S. Wang, J. Chem. Phys. 102 (1995) 2701.
[31] X.B. Wang, C.F. Ding, L.S. Wang, J. Phys. Chem. A 101 (1997) 7699.
[32] S. Li, H. Wu, L.S. Wang, J. Am. Chem. Soc. 119 (1997) 7417.
[33] X. Li, L.S. Wang, J. Chem. Phys. 111 (1999) 8389.
[34] G. Drechsler, C. Bäßmann, U. Boesl, E.W. Schlag, Z. Natforsch. A: Phys. Sci. 49 (1994) 1256.
[35] G. Drechsler, C. Bäßmann, U. Boesl, E.W. Schlag, J. Mol. Struct. 348 (1995) 337.
[36] U. Boesl, C. Bäßmann, E.W. Schlag, in: C.-Y. Ng (Ed.), Advanced Series in Physical Chemistry. Vol. 10A: Photoinization and Photodetachment, World Scientific Publishing, Singapore, 2000, p. 806.
[37] U. Boesl, C. Bäßmann, G. Drechsler, V. Distelrath, Eur. Mass Spectrom. 5 (1999) 455.
[38] U. Boesl, C. Bäßmann, R. Käsmeier, Int. J. Mass Spectrom. 206 (2001) 231.
[39] Definition of ω_e: $T_0 = \omega_e(\nu + 1/2) - \omega_e x_e(\nu + 1/2)^2$, and $\omega_e = \nu + 2\omega_e x_e$, respectively, with the measured frequency ν of the first vibrational quantum.
[40] B.K. Nash, B.K. Rao, P. Jena, J. Chem. Phys. 105 (1996) 11020.
[41] Z. Cao, J. Mol. Struct. 365 (1996) 211.
[42] R.J.H. Clark, R.G. Hester, Spectroscopy of Matrix Isolated Species, Wiley, Chichester, 1989.
[43] D.S. Moore, S.D. Robinson, Chem. Soc. Rev. 12 (1983) 415.
[44] G.G. Hladky, R.H. Crabtree, Coord. Chem. Rev. 65 (1985) 1.
[45] Z.L. Xiao, R.H. Hauge, J.L. Margrave, J. Phys. Chem. 96 (1992) 636.

[46] Z.L. Xiao, R.H. Hauge, J.L. Margrave, J. Phys. Chem. 95 (1991) 2696.
[47] A. Dedieu, Transition Metal Hydrides, VCH, Weinheim, 1992.
[48] G.A. Somorjai, Introduction to Surface Chemistry and Catalysis, Wiley, New York, 1994.
[49] G.V. Chertihin, L. Andrews, J. Phys. Chem. 99 (1995) 12131.
[50] C.E. Moore, Atomic Energy Levels, Natl. Bur. Stand. Circ. (U.S. GPO), Washington, DC, 1958.
[51] G. Herzberg, Molecular Spectra and Molecular Structure. II: Infrared and Raman Spectra of Polyatomic Molecules, Van Nostrand, New York, 1945.
[52] G.A. Ozin, D.F. McIntosh, W.J. Power, R.P. Messmer, Inorg. Chem. 20 (1981) 1782.
[53] K.P. Huber, G. Herzberg, Molecular Spectra and Molecular Structure. IV: Constants of Diatomic Molecules, Van Nostrand, New York, 1978.